Stability enhancement by joint phase measurements in a single cold atomic fountain

M. Meunier,[*] I. Dutta,[*] R. Geiger,[†] C. Guerlin,[‡] C. L. Garrido Alzar, and A. Landragin[§]

LNE-SYRTE, Systèmes de Références Temps-Espace, Observatoire de Paris, CNRS, UPMC, 61 Avenue de l'Observatoire, 75014 Paris, France

(Received 25 August 2014; published 22 December 2014)

We propose a method of joint interrogation in a single atom interferometer which overcomes the dead time between consecutive measurements in standard cold atomic fountains. The joint operation enables for a faster averaging of the Dick effect associated with the local oscillator noise in clocks and with vibration noise in cold atom inertial sensors. Such an operation allows one to achieve the lowest stability limit due to atom shot noise. We demonstrate a multiple joint operation in which up to five clouds of atoms are interrogated simultaneously in a single setup. The essential feature of multiple joint operation, demonstrated here for a microwave Ramsey interrogation, can be generalized to go beyond the current stability limit associated with dead times in present-day cold atom interferometer inertial sensors.

DOI: 10.1103/PhysRevA.90.063633 PACS number(s): 37.25.+k, 03.75.Dg, 06.30.Ft, 95.55.Sh

I. INTRODUCTION

Over the past two decades, important progress in cold atom physics has established atom interferometry (AI) as a unique tool for precision measurements of time and frequency, and of gravitoinertial effects. Atom interferometry now addresses various applications ranging from precision measurements of fundamental constants [1–3], to inertial navigation [4–6], to geophysics [7,8], and has been proposed for gravitational wave detection (see, e.g., Ref. [9]). In order to address these promising applications beyond the strict scope of atomic physics, new methods must be formulated and demonstrated experimentally to use the full potentialities of AI. The main limitation of current cold atom interferometers is dead times between successive measurements, corresponding to the preparation of the atom source and the detection of the atoms at the output of the interferometer.

In cold atom or ion clocks, dead times lead to the well-known Dick effect, where aliasing of the local oscillator noise results in a degradation of the clock short-term sensitivity [10]. Several experiments have previously demonstrated a way to bypass this effect in relative comparisons between two clocks [11–13], and in realizing a clock in the specific case of a continuous cold beam atomic source [14]. Zero-dead-time operation of two interleaved atomic clocks was recently demonstrated, resulting in a reduction of the contribution of the local oscillator noise [15]. However, besides the relevance of this proof-of-principle experiment, this method used two different atomic clocks (interrogated by the same local oscillator) and therefore requires more experimental maintenance as well as control over more systematic effects. Moreover, considering applications to inertial sensors, it is required to interrogate successive atom clouds at the same location in order to reject all parasitic inertial terms, such as centrifugal accelerations of gradients of accelerations.

Here, we propose and demonstrate a method of joint interrogation of cold atom clouds in a single atomic fountain which overcomes the dead-time limitation in atom interferometers of high sensitivity. Our joint interrogation method is inspired from atom juggling methods that were originally introduced in the context of cold atom collisions in atomic fountain clocks [16] and only realized so far for concurrent measurements [3,4,17]. With an innovative and simple control sequence, we demonstrate the simultaneous joint interrogation of up to five cold atom clouds, resulting in a long Ramsey interrogation time (800 ms), high sampling rate (up to 5 Hz), and leading to a faster reduction of the Dick effect. As cold atom inertial sensors use more than two light pulses, rejection of the Dick effect associated with vibration noise in these sensors requires more than two clouds being interrogated simultaneously in the same setup. Our multiple joint operation proposes this possibility and demonstrates it experimentally in a multiclock configuration.

II. PRINCIPLE OF THE JOINT OPERATION AND EXPERIMENTS

Most cold atom interferometers such as clocks, accelerometers, or gyroscopes are sequentially operated in a sequence of total duration T_c, and typically consist of three main steps: (i) atom trapping, cooling, and preparation; (ii) N-microwave or light-pulse AI sequence (Ramsey-like interrogation with a total duration T); and (iii) atomic state detection. Here we present experiments operating in joint mode ($T_c = T$) or multiple joint modes ($T/T_c = 2,3,4$), resulting in a null dead time and enhanced stability of the interferometer.

The normal-mode interferometer is operated sequentially following steps (i)–(iii), with an interrogation time $T =$ 480 ms and a cycle time $T_c = 900$ ms. Figure 1(b) presents the principle of the joint mode operation where the Raman interrogation pulse is shared by clouds $N-1$ (falling) and N. Figure 1(a) shows a schematic view of the experiment. Cesium atoms loaded from a two-dimensional (2D) magneto-optical trap (MOT) are trapped and cooled in a three-dimensional (3D) MOT; 4×10^7 atoms are launched vertically towards the interferometer region using moving molasses with a temperature of 1.3 μK. The launching is followed by a microwave

[*]These authors contributed equally to this work.
[†]remi.geiger@obspm.fr
[‡]Present address: Laboratoire Kastler Brossel, ENS-PSL Research University, CNRS, UPMC-Sorbonne Universités, Collège de France.
[§]arnaud.landragin@obspm.fr

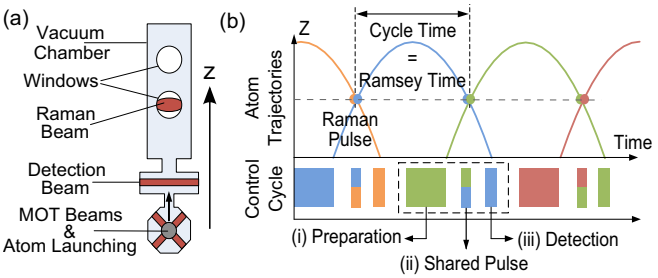

FIG. 1. (Color online) (a) Schematic of the instrument. (b) Principle of the joint mode operation: (i) Preparation of cloud N, (ii) Raman light pulse shared by clouds $N-1$ (falling) and N (rising), and (iii) detection of cloud $N-1$.

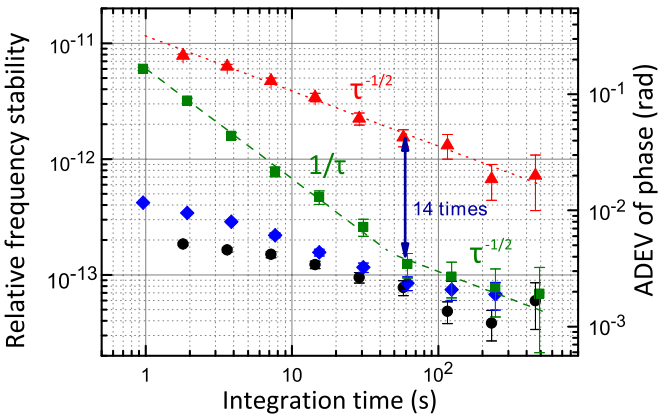

FIG. 2. (Color online) Allan deviations (ADEV) of the fountain relative frequency stability in normal and joint modes, for an interrogation time $T = 480$ ms. Stability without adding noise for the normal (black circle) and joint (blue rhombus) operations. Allan deviation for the normal mode (red triangle) and the joint mode (green square) when adding white noise over a bandwidth of 400 Hz. The $1/\tau$ (dashed) and $\tau^{-1/2}$ (dotted) lines are guide to the eyes. We observe a 14-fold gain in frequency stability from the normal to joint mode at 60 s. Integrating to this frequency stability level in a normal operation would require 12 000 s.

pulse selecting 6×10^6 atoms in the $|F = 3, m_F = 0\rangle$ state, which are used for interferometry. Light pulse interferometry is realized using copropagating Raman lasers which couple the $|F = 3, m_F = 0\rangle$ and $|F = 4, m_F = 0\rangle$ clock levels characterized by a hyperfine splitting of 9.192 GHz. Several windows enable versatile configurations for the interferometer where interrogation times up to 800 ms can be reached. In this work, we perform a Ramsey interrogation using two $\pi/2$ Raman pulses symmetric with respect to the apogee of the atom trajectory [see Fig. 1(b)]. Experimentally, the joint operation implies trapping a cloud of atoms in the bottom part of the chamber, while another atom cloud is in the interferometer or detection regions. This is a form of juggling with the clouds without recapture [16].

A microwave pulse prepares atoms in the nonmagnetic ($m_F = 0$) state before the interferometer in order to maximize the interferometer contrast. The selection is performed on the $|F = 4, m_F = +1\rangle \rightarrow |F = 3, m_F = 0\rangle$ transition, which is separated from the clock transition using a bias field of 18 mG. This scheme allows avoiding perturbation of the atoms being interrogated in the Ramsey zone by the microwave selection radiation.

With $\pi/2$ pulses of duration $\tau_p = 22$ μs (Rabi frequency $\Omega_R/2\pi = 11.4$ kHz), the phase sensitivities extrapolated at 1 s of the two-pulse Raman interferometer for the normal ($T = 480$ ms, $T_c = 900$ ms) and joint mode ($T_c = T = 480$ ms) operations are 13 and 16 mrad, respectively (see Fig. 2, black circles and blue rhombus). The sensitivity is limited by both the performance of the Raman laser phase-lock system and by the detection noise. The small difference in detection noise can be explained by a fringe contrast loss from 50% to 30% when implementing the joint operation. This contrast loss originates from stray light scattered from the MOT atoms which interacts with the atoms in the interferometer region, starting 0.5 m above, transferring them in unwanted states. Moreover, this stray light induces a light shift on the interference fringes (see Appendix, Fig. 5). The effects of the MOT scattered light could be suppressed with the use of a vacuum-compatible controllable shutter [18] between the MOT and interrogation regions.

III. REJECTION OF THE LOCAL OSCILLATOR NOISE IN JOINT OPERATION

The phase of the two-pulse atom interferometer is determined by the Raman laser phase difference imprinted on the atomic wave function at the light pulses; at time t_i it reads $\Delta\Phi_i = \phi(T + t_i) - \phi(t_i)$, where $\phi(t)$ is the Raman laser relative phase. In the case of a white relative phase noise and after N cycles, the variance $\langle \Delta\Phi_N^2 \rangle$ of the accumulated atomic phase is inversely proportional to N. In the time domain, this means that the phase Allan deviation scales as $1/\sqrt{\tau}$ (τ is the integration time), which is the well-known result for successive uncorrelated measurements. With the cycle time T_c equal to the Ramsey time T, the second laser pulse $\phi(T + t_i)$ of cloud i is the same as the first pulse $\phi(t_{i+1})$ of cloud $i + 1$: $\phi(T + t_i) = \phi(t_{i+1})$. As a result, the consecutive phase terms in the accumulated atomic phase cancel each other, so that the variance of the accumulated phase $\langle \Delta\Phi_N^2 \rangle$ scales as $1/N^2$ (Allan deviation of phase $\sim 1/\tau$). In other words, the joint operation rejects the aliasing of the local oscillator noise (here the Raman laser relative phase noise) usually encountered when performing independent measurements of the phase with dead times. The rejection applies as long as the local oscillator noise spectrum has a bandwidth that is lower than the pulse Rabi frequency Ω_R. We quantitatively analyze the rejection efficiency below.

To demonstrate the local oscillator (LO) phase noise rejection, we introduce a white noise of controlled amplitude and bandwidth in the Raman laser phase-lock loop. The noise is generated using a direct digital synthesizer (SRS DS345) and filtered by an analog 115 dB/octave low-pass filter (SR 650). The spectrum of added noise and the details of its calibration

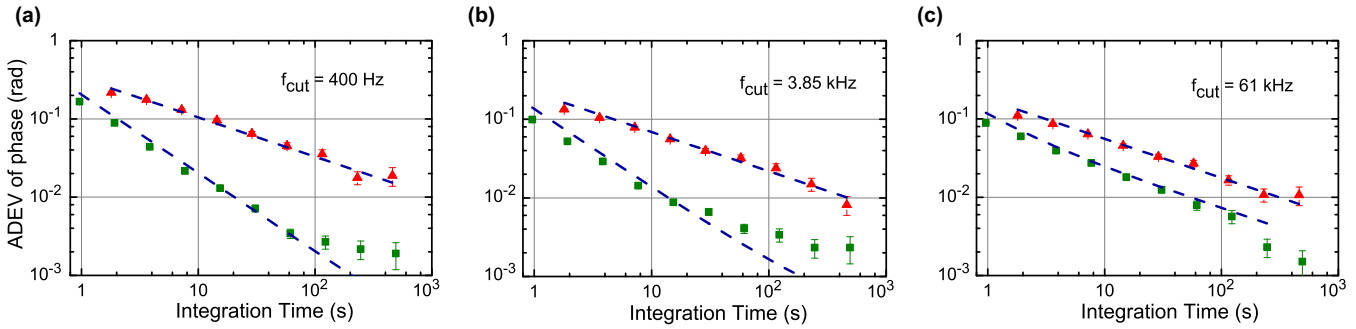

FIG. 3. (Color online) Comparison of the normal mode (red triangles) and joint mode (green squares) for several cutoff frequencies $f_{\rm cut}$ of added white noise to the Raman laser phase-lock loop: (a) 400 Hz, (b) 3.85 kHz, and (c) 61 kHz. The Raman pulse Rabi frequency is $f_R = 11.4$ kHz. Dashed blue lines: Theoretical calculation based on Eq. (1) without a free parameter.

are given in Appendix, Fig. 6. Figure 2 shows the measured phase Allan deviation (ADEV) for a white noise of 400 Hz bandwidth (green squares), well below the Rabi frequency of 11.4 kHz. We clearly observe the expected $1/\tau$ scaling of the joint operation. A change of slope in the ADEV is observed at 60 s when reaching the uncorrelated noise floor at a level of 1×10^{-13} in relative frequency stability, corresponding to detection noise. Figure 2 thus shows that the joint operation allows for fast averaging to the fundamental noise linked to the detection noise, even with a low stability local oscillator.

The joint operation efficiently rejects the Dick effect associated with low frequencies in the LO noise, but the rejection is less efficient for LO noise bandwidths $f_{\rm cut}$ that are higher than the Raman pulse Rabi frequency $f_R = \Omega_R/2\pi$. In the following we explore the limits of the rejection. Figure 3 presents phase ADEV for measurements corresponding to LO noise bandwidths of 400 Hz [Fig. 3(a)], 3.85 kHz [Fig. 3(b)], and 61 kHz [Fig. 3(c)]. The $1/\tau$ region expands over longer interrogation times for $f_{\rm cut} = 400$ Hz than for $f_c = 3.85$ kHz. In the latter case, the Allan deviation changes its slope after $\sim$10 s of integration time. In the 61 kHz case, the $1/\tau$ scaling is no longer visible: The joint mode no longer samples the LO noise so that correlation does not exist between successive measurements.

To quantitatively analyze our data, we use the AI sensitivity function formalism, which provides the response of the atom interferometer to a perturbation at a given frequency [19,20]. The Allan variance of the phase reads

$$\sigma^2(\tau) = \frac{1}{2m^2}\int_0^{+\infty}\frac{d\omega}{2\pi}|H(\omega)|^2 S_\phi(\omega)\frac{4\sin^4(m\omega T_c/2)}{\sin^2(\omega T_c/2)}, \quad (1)$$

where $|H(\omega)|^2$ is the interferometer sensitivity function, $S_\phi(\omega)$ is the noise power spectral density of the Raman laser relative phase, and $\tau = mT_c$; m is therefore the number of averaged samples in the calculation of the Allan variance. The two-pulse inteferometer sensitivity function is given by [19,20]

$$|H(\omega)|^2 = \frac{4\omega^2\Omega_R^2}{\left(\omega^2-\Omega_R^2\right)^2}\left[\cos\omega\left(\frac{T}{2}+\tau_p\right)+\frac{\Omega_R}{\omega}\sin\frac{\omega T}{2}\right]^2, \quad (2)$$

with τ_p the duration of the Raman $\pi/2$ pulse. Using the measured white Raman phase noise levels $S_\phi(\omega) = S_0$ (Fig. 6) and evaluating Eq. (1) numerically, we obtained the dashed lines in Figs. 3(a)–3(c) for the normal mode ($T_c = 900$ ms, $T = 480$ ms) and for the joint mode ($T_c = T + \tau_p$). Our calculation reproduces well the experimental results, without a free parameter. In particular, the change of slope from τ^{-1} to $\tau^{-1/2}$ is well captured. It occurs at the point in time

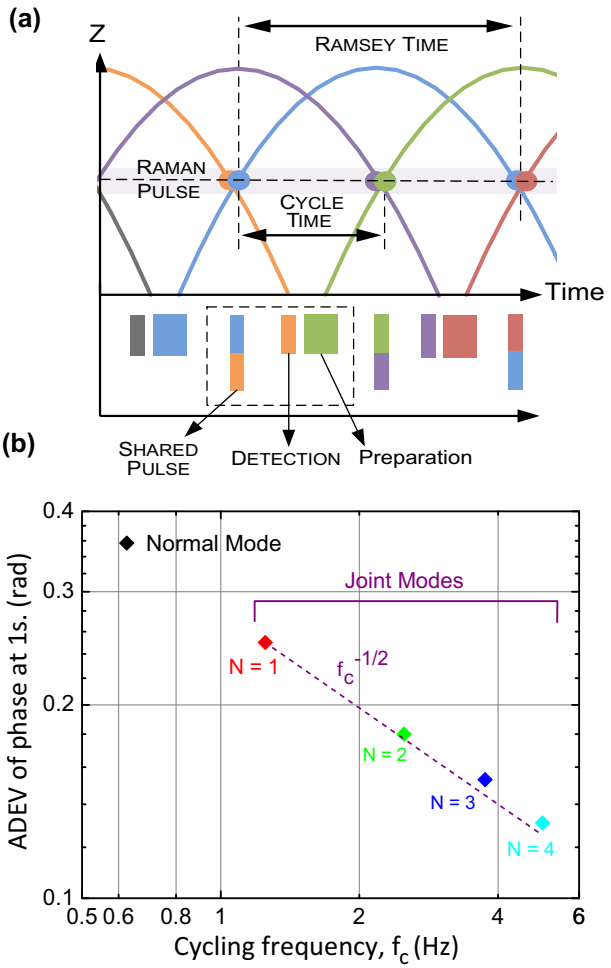

FIG. 4. (Color online) (a) Schematic of the double joint operation where $T/T_c = 2$, where three atom clouds simultaneously interact with the Raman laser pulses. (b) Short-term sensitivity at 1 s for each of the operation modes and $T = 801$ ms, from the normal operation ($T_c = 1.6$ s) to the quadrupole joint mode ($T/T_c = 4$). The dashed line is a guide to the eye showing the $1/\sqrt{f_c}$ scaling.

when the contribution of the high-frequency noise ($f_{\rm cut} > f_R$) starts overcoming the low-frequency noise contributions ($f_{\rm cut} < f_R$), which are well correlated in successive joint measurements.

IV. MULTIPLE JOINT OPERATION

We now present the extension of our method to a multiple joint operation where we interleave more than two atom interferometry measurements. This ability is essential to reject the Dick effect associated with vibration noise in cold atom inertial sensors which use more than two light pulses to build the interferometer and thus require more than two clouds being jointly interrogated. The agility of our experimental setup allows us to further enhance the interferometric sensitivity by juggling with more than two atom clouds, resulting in a cycle time T_c being a submultiple of the Ramsey time T. Increasing T to 801 ms, we present four configurations of the joint operation with $T/T_c = 1$–4. Figure 4(a) presents the principle of the double joint configuration where $T/T_c = 2$. To characterize the sensitivity gain of the multiple joint operation, we proceed as before by introducing a 400 Hz bandwidth white noise to the Raman laser phase-lock loop. For the four different configurations of $T_c = [801,400.5,267,200.25]$ ms, we observed a similar $1/\tau$ scaling of the phase ADEV in the different joint modes. Figure 4(b) shows the short-term sensitivity at 1 s versus the cycling frequency $f_c = 1/T_c$. For the single joint mode interferometer with $T = 801$ ms, the short-term phase sensitivity is 250 mrad, while it is 131 mrad in a quadrupole joint mode. This demonstrates a sensitivity enhancement of 1.9 close to the expected value $(f_c^{\rm quad}/f_c^{\rm single})^{1/2} = 2$.

The minimum value of the cycle time in the multiple joint mode is limited by the duration of preparation of the cold atoms. In our setup, we used a 150-ms-long MOT loading stage where the detection noise is at the limit between quantum projection noise and technical noise. Going beyond could be achieved with optimum loading of the MOT.

V. CONCLUSION

We have demonstrated a method for operating an atom interferometer in a joint configuration where five atom clouds are interrogated simultaneously by common interrogation lasers. Our method highly rejects the Dick effect present in standard atomic fountains operated with dead times. It enables faster averaging of the phase noise to achieve the fundamental noise floor linked to the detection noise. This method remains efficient as soon as the noise frequency components are below the pulse Rabi frequency. We also demonstrated an extension of this method to a multiple joint scheme, where several interleaved interrogations result in further improvement of the stability.

The joint method enables one to run microwave frequency standards at the best performances (i.e., at the quantum projection noise limit) without sophisticated and expensive ultrastable oscillators [21–23] by canceling the Dick effect (and increasing the locking bandwidth of the local oscillator). Our method can be directly used for the rejection of parasitic vibrations in cold atom inertial sensors operated with dead times. In such systems, in which the signal is fluctuating, dead times not only reduce drastically the stability but lead to loss of information [24]. Moreover, the multiple joint operation gives access to high-frequency components while maintaining high sensitivity linked to long interaction times achievable with cold atom sensors.

ACKNOWLEDGMENTS

We thank Bertrand Venon, Thomas Lévèque, David Horville, and Michel Lours for their contributions to the design of the experiment and the first stages of the realization, and Denis Savoie for his contribution to the simulations. We thank DGA (Délégation Génerale pour l'Armement), IFRAF (Institut Francilien de Recherche sur les Atomes Froids) for funding. M.M was supported by Délégation Générale pour l'Armement (DGA), and I.D. by Centre National d'Etudes Spatiales (CNES) and LABEX Cluster of Excellence FIRST-TF (ANR-10-LABX-48-01) within the Program "Investissements d'Avenir" operated by the French National Research Agency (ANR).

APPENDIX

A. Influence of the light scattered by the atoms in the MOT

See Fig. 5.

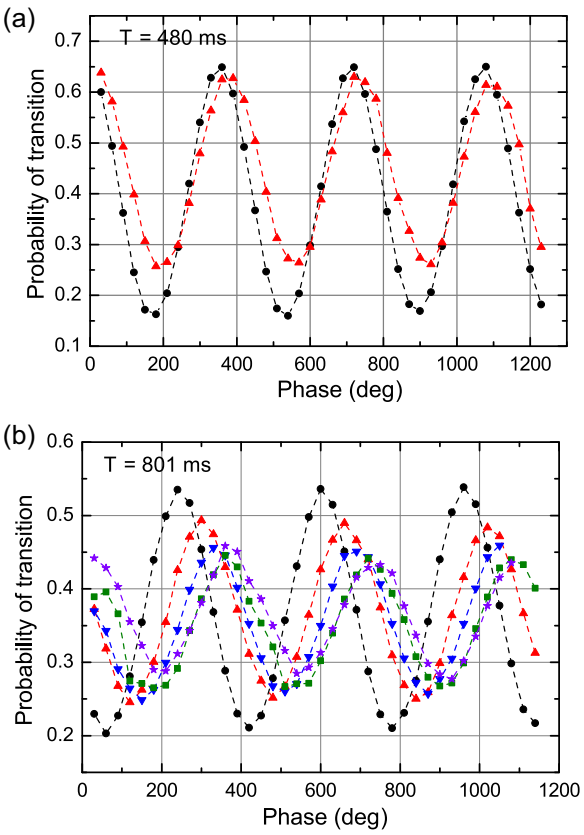

FIG. 5. (Color online) Interference fringes for two different Ramsey interrogation times: (a) $T = 480$ ms for the normal (black dots) and joint (red triangles) modes; (b) $T = 801$ ms for the normal (black dots), joint (red triangles), and multiple joint operations (double joint: blue triangles; triple joint: green squares; quadrupole joint: violet stars).

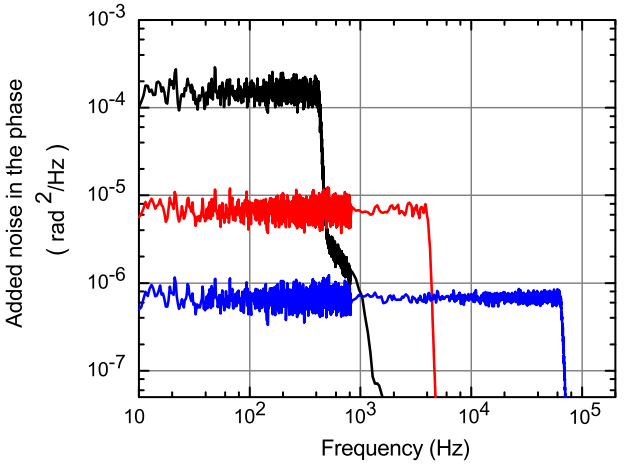

FIG. 6. (Color online) Power spectral density of the white added noise for the three different values of f_{cut}. Black (top) $f_{\text{cut}} = 400$ Hz; red (middle) $f_{\text{cut}} = 3.85$ kHz; blue (bottom) $f_{\text{cut}} = 61$ kHz.

B. Added Raman laser phase noise

The white noise was generated using a direct digital synthesizer (SRS DS345) and filtered by an analog 115 dB/octave low-pass filter (SR 650), and directly added to the Raman laser phase-lock loop. The spectrum of the added noise is given in Fig. 6. Its exact calibration was important for the quantitative analyses presented in Fig. 3 of the main text. To calibrate the noise level, we applied a sinusoidal modulation of known amplitude (in volts) and frequency (0.1 Hz) to the Raman laser phase-lock loop and measured the corresponding modulation of the interferometer phase (in radians). This yielded the conversion factor from volts to radians and the following white-noise levels: $S_0 = 1.5 \pm 0.3 \times 10^{-4}$ rad^2/Hz for 400 Hz; $S_0 = 6.8 \pm 1.4 \times 10^{-6}$ rad^2/Hz for 3.85 kHz; and $S_0 = 6.7 \pm 1.3 \times 10^{-7}$ rad^2/Hz for 61 kHz. These measured noise levels were used in Eq. (1).

[1] J. Guéna, M. Abgrall, D. Rovera, P. Rosenbusch, M. E. Tobar, P. Laurent, A. Clairon, and S. Bize, Phys. Rev. Lett. **109**, 080801 (2012), and references therein.

[2] R. Bouchendira, P. Cladé, S. Guellati-Khelifa, F. Nez, and F. Biraben, Ann. Phys. **525**, 484 (2013).

[3] G. Rosi, F. Sorrentino, L. Cacciapuoti, M. Prevedelli, and G. M. Tino, Nature (London) **510**, 518 (2014).

[4] B. Canuel, F. Leduc, D. Holleville, A. Gauguet, J. Fils, A. Virdis, A. Clairon, N. Dimarcq, C. J. Bordé, A. Landragin *et al.*, Phys. Rev. Lett. **97**, 010402 (2006).

[5] R. Geiger, V. Ménoret, G. Stern, N. Zahzam, P. Cheinet, B. Battelier, A. Villing, F. Moron, M. Lours, Y. Bidel, A. Bresson, A. Landragin, and P. Bouyer, Nat. Commun. **2**, 474 (2011).

[6] B. Barrett, P.-A. Gominet, E. Cantin, L. Antoni-Micollier, A. Bertoldi, B. Battelier, P. Bouyer, J. Lautier, and A. Landragin, in *Atom Interferometry, Proceedings of the International School of Physics "Enrico Fermi," Course CLXXXVIII, Varenna, 2013*, edited by G. M. Tino and M. A. Kasevich (IOS, Amsterdam, 2014), p. 493.

[7] Z. Jiang, V. Palinkas, F. E. Arias, J. Liard, S. Merlet, H. Wilmes, L. Vitushkin, L. Robertsson, L. Tisserand, F. Pereira Dos Santos *et al.*, Metrologia **49**, 666 (2012).

[8] P. Gillot, O. Francis, A. Landragin, F. Pereira Dos Santos, and S. Merlet, Metrologia **51**, L15 (2014).

[9] S. Dimopoulos, P. W. Graham, J. M. Hogan, M. A. Kasevich, and S. Rajendran, Phys. Rev. D **78**, 122002 (2008).

[10] G. J. Dick, J. D. Prestage, C. A. Greenhall, and L. Maleki, in *Proceedings of the 22nd Annual Precise Time and Time Interval (PTTI) Applications and Planning Meeting*, edited by R. L. Sydnor (NASA, Hampton, VA, 1990), pp. 487–508, http://oai.dtic.mil/oai/oai?verb=getRecord&metadataPrefix=html&identifier=ADA515721.

[11] S. Bize., Y. Sortais, P. Lemonde, S. Zhang, P. Laurent, G. Santarelli, C. Salomon, and A. Clairon, IEEE Trans. Ultrason. Ferroelectr. Freq. Control **47**, 1253 (2000).

[12] M. Takamoto, T. Takano, and H. Katori, Nat. Photonics **5**, 288 (2011).

[13] C. W. Chou, D. B. Hume, M. J. Thorpe, D. J. Wineland, and T. Rosenband, Phys. Rev. Lett. **106**, 160801 (2011).

[14] L. Devenoges, A. Stefanov, A. Joyet, P. Thomann, and G. Di Domenico, IEEE Trans. Ultrason. Ferroelectr. Freq. Control **59**, 211 (2012).

[15] G. W. Biedermann, K. Takase, X. Wu, L. Deslauriers, S. Roy, and M. A. Kasevich, Phys. Rev. Lett. **111**, 170802 (2013).

[16] R. Legere and K. Gibble, Phys. Rev. Lett. **81**, 5780 (1998).

[17] Z.-K. Hu, X.-C. Duan, M.-K. Zhou, B.-L. Sun, J.-B. Zhao, M.-M. Huang, and J. Luo, Phys. Rev. A **84**, 013620 (2011).

[18] F. Füzesi, A. Jornod, P. Thomann, M. D. Plimmer, G. Dudle, R. Moser, L. Sache, and H. Bleuler, Rev. Sci. Instrum. **78**, 103109 (2007).

[19] P. Lemonde, G. Santarelli, P. Laurent, F. Pereira dos Santos, A. Clairon, and C. Salomon, in *Proceedings of the 1998 IEEE International Frequency Control Symposium* (IEEE, Piscataway, NJ, 1998), pp. 110–115.

[20] P. Cheinet, B. Canuel, F. Pereira Dos Santos, A. Gauguet, F. Leduc, and A. Landragin, IEEE Trans. Instrum. Meas. **57**, 1141 (2008).

[21] S. Grop, P.-Y. Bourgeois, R. Boudot, Y. Kersalé, E. Rubiola, and V. Giordano, Electron. Lett. **46**, 420 (2010).

[22] J. G. Hartnett, N. R. Nand, and C. Lu, Appl. Phys. Lett. **100**, 183501 (2012).

[23] Ultra Low Instability Signal Source, http://www.uliss-st.com/.

[24] C. Jekeli, Navigation **52**, 1 (2005).